

## Preparation and characterization of ultrafiltration membranes embedded with ZIF-8 metal-organic framework particles for oil removal from aqueous solutions

Ghaidaa S. Hassoon<sup>1</sup>, Shaalan B. Ahmed<sup>1</sup>, Athar S. Mteran<sup>1</sup>,  
Wafaa Kh. Al-Musawy<sup>1</sup>, Manar A. Ehmud<sup>1</sup> , Mustafa H. Al-Furajji<sup>\*1</sup> 

<sup>1</sup> Water, Environment, and Renewable Energy Center, Scientific Research Commission, Ministry of High Education and Scientific Research, Baghdad, Iraq

\* Corresponding author's e-mail: [alfurajji79@gmail.com](mailto:alfurajji79@gmail.com)

### ABSTRACT

The growth of nanotechnology has sparked a new wave of interest in membrane technologies, particularly due to the invention of nanocomposite membranes. Zeolitic imidazolate frameworks (ZIF-8), a subclass of metal-organic frameworks (MOF) materials known for their chemical and thermal stability, were incorporated into polysulfone (PSU) ultrafiltration membranes for the removal of oil from water. Nanocomposite PSU-ZIF-8 membranes were prepared by adding varying amounts of ZIF-8 nanoparticles (0.025, 0.05, and 0.075 wt%) into the polymeric PSU solution. The membranes were characterized by contact angle (CA), X-ray diffraction (XRD), Fourier-transform infrared spectroscopy (FTIR), field emission scanning electron microscopy (FE-SEM), and porosity analysis. The highest porosity, 70%, was observed for the PSU/ZIF-8-0.05 wt.% membrane. The porosity was used to assess the membrane's performance in terms of fluid passage and selective filtration efficiency. Membranes with and without ZIF-8 were tested for flux and oil rejection. The PSU membrane without ZIF-8 showed a flux of 50 L/m<sup>2</sup>·h and 86% oil rejection. With the addition of ZIF-8, the flux increased, with the PSU/ZIF-8-0.025 wt.% membrane achieving 53.57 L/m<sup>2</sup>·h and 87% oil rejection. Performance continued to improve with higher ZIF-8 concentrations, with peak performance reached at 0.05 wt.% ZIF-8, which resulted in enhanced flux and oil rejection efficiency.

**Keywords:** membrane, metal-organic frameworks, zeolitic imidazolate frameworks, ultrafiltration, oily wastewater.

### INTRODUCTION

Oily wastewater comprises fats, oils, greases, and dissolved organic and/or inorganic substances in suspension (Yu et al., 2017). Various industries, including metal processing, edible oil refineries, petrochemical industries, tannery industries, etc., produce oil-contaminated wastewater. Several methods are used to process and remove oil from polluted water (Al-Jadir et al., 2022; Zhao et al., 2021). Include physical techniques like sedimentation, filtration, and clarity; chemical techniques like flocculation/coagulation, chemical disinfection, and distillation; and biological techniques like microbial treatment to eliminate pollutants (Cococceanu & Man, 2021). Certain traditional methods work

well for treating wastewater at its primary stage, separating solid sludge from the wastewater and removing soil contaminants and naturally occurring organic matter (G. Li et al., 2018). Advanced approaches to treatment are required for substances that cannot be separated using typical methods during the initial phase of treatment (Parsons, 2004). These techniques include enhanced oxidation processes, membrane-based techniques, and adsorption technologies. Adsorption-based methods is the process in which an ion or molecule from a liquid or gaseous bulk-phase clings to a solid surface (Rathi & Kumar, 2021). There are two possible ways that water contaminants can adsorb on sorbent materials: chemisorption or physisorption (Mulay & Martsinovich, 2023). Advanced oxidation refers

to chemical oxidation using hydroxyl radicals, which are highly reactive and short-lived oxidants. The radicals must be created on-site in a reactor where they may interact with the organics in the waste product (Deng & Zhao, 2015). Nature-based techniques entail using natural aggregates to remove pollution. For example, a natural process is phytoremediation. These ways utilize layers of organic materials to filter wastewater (Rozkošný et al., 2014). Membrane-based methods are further kind based on the type and size of the membrane. Commercially available membrane-based processes include nanofiltration (NF), microfiltration (MF), ultrafiltration (UF), and reverse osmosis (a pressure-based approach (Singh & Hankins, 2016). The effectiveness of membrane-based methods is dependent on the size of the membrane pores and the size of the pollutants, the chemical and thermal stability of membranes and pollutants, the reusability of membranes, and their selectivity towards pollutant removal (Nawaz et al., 2016). Membrane-based techniques are efficient in eliminating contaminants of various sizes. Although ultrafiltration is good at removing viruses and natural organic matter (NOM), nanofiltration effectively removes certain salts. It has also been used to remove color from textile wastewater (Ji et al., 2017). Microfiltration may be helpful for the removal of some microorganisms, clay particles, and microplastics (Dasgupta et al., 2015) The permeability and selectivity of the polymeric membranes hindered their performance. MOFs, nano-silica, zeolite 4A etc. can be incorporated in membrane matrix to improve membrane performance (Al-Furaiji et al., 2018) Therefore, adding nanofillers such as metal oxides. A subclass of MOFs, zeolitic imidazolate frameworks (ZIFs) are emerging as a novel class of molecular sieves with extremely variable and diversified structural characteristics and low cost. ZIFs, which were made from three-dimensional arrays of tetrahedral metallic ions joined by organic ligands, were distinguished by their high crystalline nature and porous structure (Beauregard

et al., 2020) .Several analytical methods, including FT-IR, XRD, SEM, AFM, and contact angle analysis, were used to investigate the physical and chemical properties of the produced materials. This study aims to enhance the performance of polysulfone (PSU) ultrafiltration membranes by adding ZIF-8 nanoparticles and examining how they affect the shape of membranes and the effectiveness of oil removal from aqueous solutions. Finding the ideal ZIF-8 concentration to increase flux and separation efficiency.

## MATERIALS AND METHODS

### Materials

Polysulfone with a molecular weight of 22,000 g/mol was ordered from Xi'an Lyphar Biotech Co., Ltd., China. N, N-dimethylformamide (DMF, Mw = 73.1 g/mol), as a solvent, was purchased from Thomas Baker (Chemicals) Pvt. Ltd. (Mumbai, India). Tween 80 was obtained from Hopkin & Williams Ltd. (Wolverhampton, UK), while the midland Iraqi refineries company provided kerosene. Zinc nitrate hexahydrate from SRL (Sisco Research Laboratories)-India, Methanol from Hayman-UK, 2-methylimidazole from Sigma-Aldrich (Kenilworth, NJ, USA) and a locally fabricated system (Table 1).

### Preparation of MOFs-ZIF-8

First, 2-methylimidazole (1.313 g in 10 ml methanol) and zinc nitrate hexahydrate (0.594 g in 10 ml methanol) were separately dissolved in methanol. ZIF-8 particle generation was then carried out in an ice bath while being agitated at a speed of 250 rpm after 10 mL of zinc nitrate hexahydrate solution was added to 10 mL of 2-methylimidazole solution. After ten minutes, the reaction was stopped by adding 100 milliliters of methanol to the reaction mixture. The generated ZIF-8 particles were separated from the reaction mixture by centrifugation, which

**Table 1.** Synthesized membrane composition

Membrane	PSU wt. %	DMF wt. %	ZIF-8 (g)
ZIF-8-0	14%	86	0
ZIF-8-0.025	14%	86	0.0025
ZIF-8-0.005	14%	86	0.005
ZIF-8-0.0075	14%	86	0.0075

was run for 20 minutes at 8000 rpm. To get rid of the unreacted reactants, the ZIF-8 particles underwent two cycles of centrifugation and methanol washing. In the end, ZIF-8 particles were created and kept for further use.

### Preparation of UF membranes

The PSU UF membranes used in this research were prepared using the phase inversion method. Firstly, the casting solution was prepared by dissolving the appropriate amount of PSU in DMF solvent in a weight ratio of 14%. The obtained mixture was stirred for 6 h at 60 °C and left overnight for degassing at room temperature. Then, the casting polymeric solution was poured on a clean glass plate and cast using a casting Gardner knife (Filmography: film casting doctor blade) at a thickness of 180  $\mu\text{m}$ . The glass plate with the polymeric solution was then immersed directly in a water bath at room temperature. The flat sheet PSU membrane was detached in a few seconds from the glass plate and stored in DI water at 4 °C before testing. The PSU-MOFs ZIF-8 membranes were prepared using the same procedure, except the appropriate amount of the MOFs ZIF-8 nanoparticles was added to the casting solution before the phase inversion method.

### Preparation for oily wastewater

0.5 g of kerosene was measured and mixed with 1000 mL of distilled water to create a kerosene-in-water emulsion. A few drops of Tween 80 were added to the mixture to improve emulsification. To guarantee that the kerosene droplets were well distributed throughout the aqueous phase, the mixture was stirred for five minutes using a mechanical stirrer.

### Characterization

The chemical composition of the generated membranes was ascertained using the Fourier transform infrared-attenuated total reflection (FTIR) (Thermo Scientific Nicolet iS20 (USA)) method. A scanning electron microscope (SEM) (TESCAN MIRA3 FRENCH) was used to display the morphological microstructure of the produced membranes and the ZIF-8 NPs. AFM (Angstrom Advanced Inc., 2008, U.S.A.) was utilized to determine the produced membranes' surface roughness. A gravimetric technique was used to assess the membrane sample's porosity. The diameters and zeta potentials

of the ZIF-8 NPs were measured using the zeta plus analyzer, Brookhaven, USA. Powder X-ray diffraction (XRD) patterns were recorded using an X-ray diffractometer (XRD 6000/SHIMADZU, Japan), theta light (TL100 and TL101)-Finland, UV-VIS from biotech engineering management (UK).

## RESULTS AND DISCUSSION

### Results of ZIF-8 and UF membranes tests

We successfully generated ZIF-8 NPs. An SEM image of the ZIF-8-produced nanoparticles with a regular shape can be seen in Figure 1. The ZIF-8 sample is shown in Figure 1, where it is evident that the particles were dispersed across the entire film thickness. This sample showed both small and big particles. This investigation revealed a diameter of approximately 59.120, 50.228, 50.139, and 45.263 nm. The ligand is responsible for the nitrogen atoms present in the ZIF-8 structure. A cubic crystal system with space group number 217 (I-43m) is revealed for the compound, and the peaks showed a good match, confirming that ZIF-8. The material's crystallinity was ascertained using XRD Figure 2, which yielded crystallographic data typical of zeolitic imidazolate frameworks. The chemical formula,  $\text{Zn}_{12.00}\text{N}_{48.00}\text{C}_{75.60}\text{H}_{79.80}$ , shows a different stoichiometry than the conventional ZIF-8 (Arunachalam et al., 2021). The XRD result showed that the sample is mostly composed of carbon and nitrogen with trace levels of zinc. According to Figure 2, the XRD pattern displays peaks at  $2\theta$  of  $26.3^\circ$  and  $29.7^\circ$  that correspond to

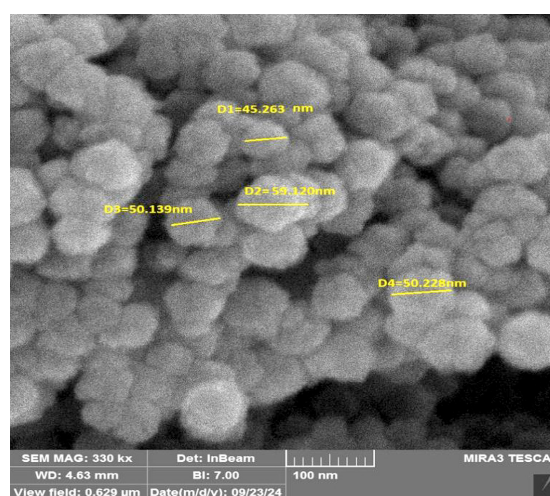


**Figure 1.** SEM images of the surface structure and the morphology

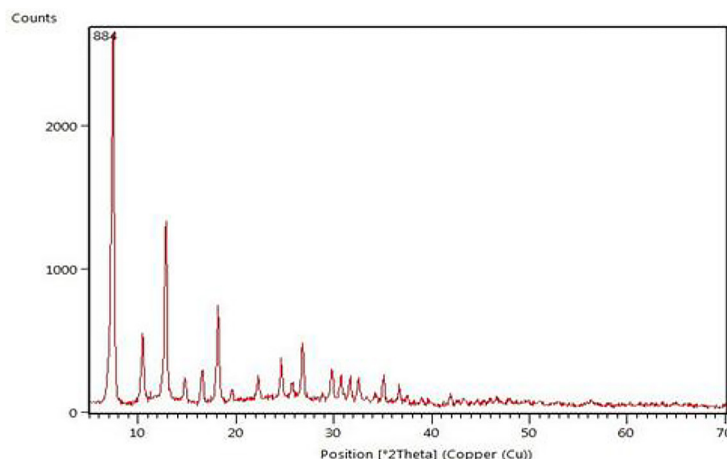


Figure 2. XRD analysis of ZIF-8 nanoparticles

the reflection planes (011) and (112), respectively. These peaks are all crystalline features of phase formation. The size of the formed crystallites ( $D$ ) can be calculated by the Debye–Scherrer equation (Vinila et al., 2014):

$$D = k \lambda / \beta \cos \theta \quad (1)$$

where:  $D$  – the average grain size,  $k$  – a numerical factor frequently referred to as the crystallite-shape factor (taken as 0.9),  $\lambda$  – the wavelength of the X-rays,  $\beta$  – the width (full-width at half-maximum) of the X-ray diffraction peak in radians,  $\theta$  – the Bragg angle.

The SEM images demonstrate the formation of regular-shaped nanoparticles of the synthesized ZIF-8. This study also revealed that, in addition to the regular spherical shape, the particles are packed in a regular spherical shape, and they have a structure. Figure 3 also shows the findings of the examination of the atomic energy microscope (AFM), and it seems that the AFM image of the ZIF-8 particles in two and three dimensions is displayed

there. As seen in Figure 4, ZIF-8 nanoparticles (NPs) exhibit a zeta potential of -39.53 mV, indicating that their dispersion is extremely stable. The Zeta-Potential measures the electrostatic repulsion between particles; a high value indicates strong repulsive forces, which often aid in maintaining colloidal stability by preventing aggregation. In this case, ZIF-8 NPs most likely have a strong ability to remain disseminated in solution due to their positive surface charge (Costa et al., 2023).

As shown in Figure 5 the morphological evaluation of polysulfone membrane with and without ZIF-8 shows notable structural variations in cross-sectional and surface characteristics. The comparatively smooth and dense surface appearance of the polysulfone membranes (A and C) is typical of phase-inversion membranes. The cross-sectional SEM picture (C) displays an asymmetric structure with a porous sublayer made up of spaces that resemble fingers and a dense top layer. With the porous support improving mechanical stability and water transport and the dense skin layer controlling separation performance, this shape guarantees a

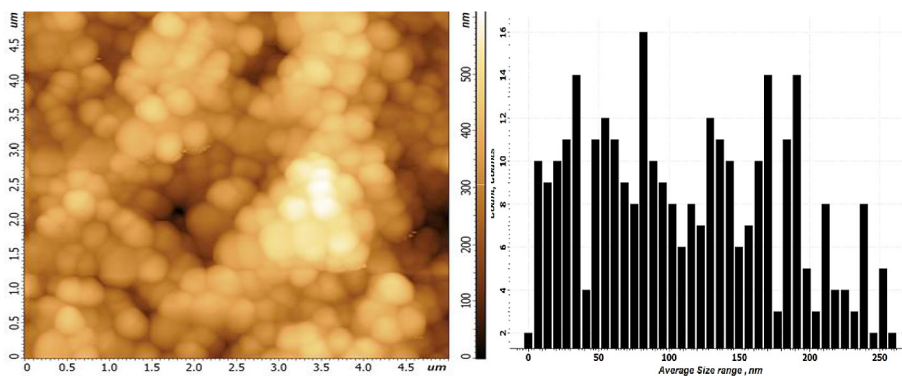
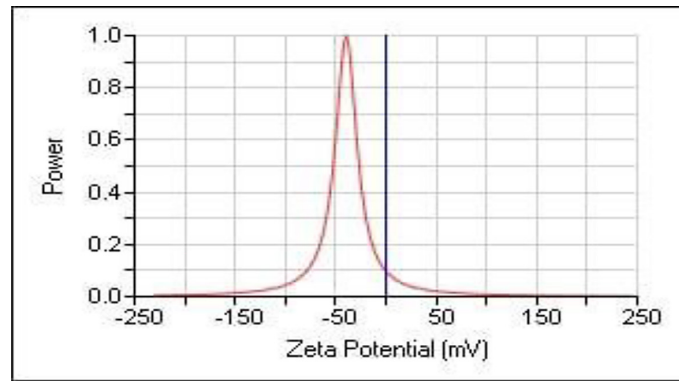
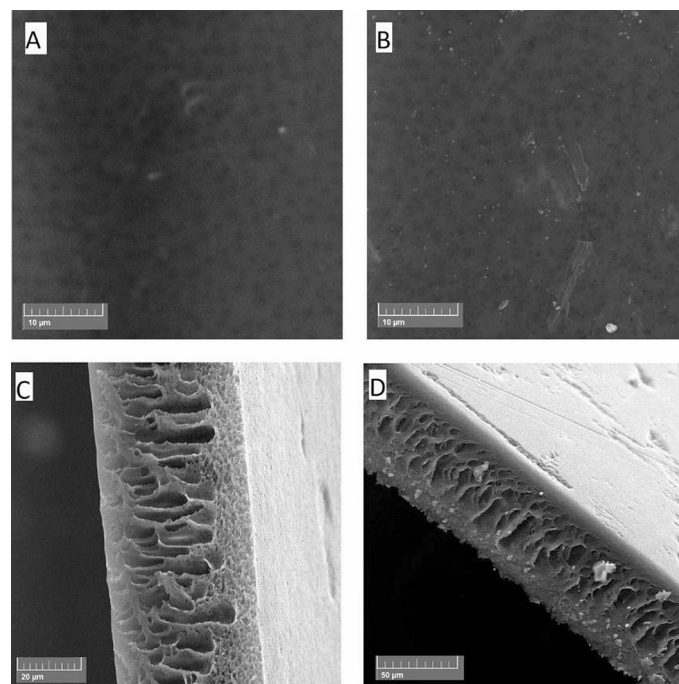


Figure 3. AFM scan showing top surface topography of ZIF-8 nanoparticles



**Figure 4.** Zeta potential of ZIF-8 nanoparticles



**Figure 5.** SEM images of polysulfone membranes: (A, C) pristine polysulfone membranes without ZIF-8, (B, D) polysulfone membranes with ZIF-8 incorporation cross section

balance between selectivity and permeability. The presence of scattered nanoparticles within the polymer matrix causes the surface morphology (B) to become rougher upon the addition of ZIF-8 (B and D). The hydrophilicity, water affinity, and antifouling qualities can all be improved by this increased surface roughness. In contrast to the pristine membrane, the membrane structure shows bigger and more linked pores in the cross-sectional image (D). ZIF-8 promotes pore formation and increases water permeability by influencing phase separation during membrane manufacturing. However, too much ZIF-8 loading might cause partial pore blockage or nanoparticle aggregation, which can lower the effective permeability area and affect filtration efficiency.

These morphological changes suggest that ZIF-8 is essential for modifying the porosity of membranes, surface characteristics, and overall filtering effectiveness. To optimize performance without sacrificing membrane integrity, ZIF-8 concentration must be properly optimized (Mei et al., 2020).

## FTIR ANALYSIS

The Fourier transmission infrared spectrometer is an essential chemical characterization method for identifying the functional groups contained in a substance. The surface of the pristine PSU 14% membrane and the composite membranes with the

addition of ZIF-8 nanoparticles were compared using FTIR-ATR analysis, as shown in Figures 6, 7, and 8. As shown in Figure 6 The Zn-N stretching vibration is identified in the literature as being about  $420.48\text{ cm}^{-1}$  in the FTIR spectra of clean ZIF-8, followed by the C-N stretching vibration at  $1141.86\text{ cm}^{-1}$  and the C-C in-stretching vibration at  $1583.56\text{ cm}^{-1}$ . Peaks at  $2926.01\text{ cm}^{-1}$  (aromatic) and  $3126.61\text{ cm}^{-1}$  aliphatic of C-H  $\text{cm}^{-1}$  stretching and  $1583\text{ cm}^{-1}$  emerge of C=N (Zhang et al., 2018).

Peaks at  $1494.83\text{ cm}^{-1}$  and  $1585.49\text{ cm}^{-1}$  (C-C ring stretching vibration),  $1298.09\text{ cm}^{-1}$  (O=S=O

asymmetric stretching vibration),  $124.16\text{ cm}^{-1}$  (C-O stretching vibration),  $1157.29\text{ cm}^{-1}$  (O=S=O Ring symmetric vibration), and  $1012\text{ cm}^{-1}$  (aryl groups) are visible in the FTIR spectra of the polysulfone membranes in Figure 7 (Arunachalam et al., 2021). Figure 8 displays the PSU/ZIF-8 membrane's FTIR spectra. The primary peaks of ZIF-8 are situated at  $1157\text{ cm}^{-1}$ , ascribed to the C-N stretching, and  $1585.49\text{ cm}^{-1}$ , assigned to the C=N stretching. The distinct stretching of Zn-N and Zn-o is represented by the  $422.41$  and  $464.84\text{ cm}^{-1}$  peaks, respectively (Tsai & Langner, 2016).

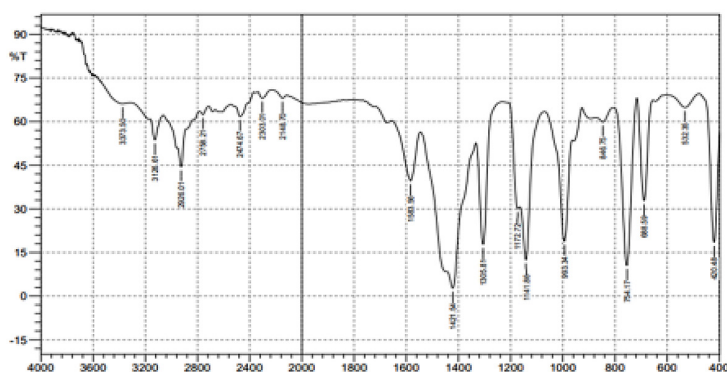


Figure 6. FTIR (ZIF-8) nanoparticles

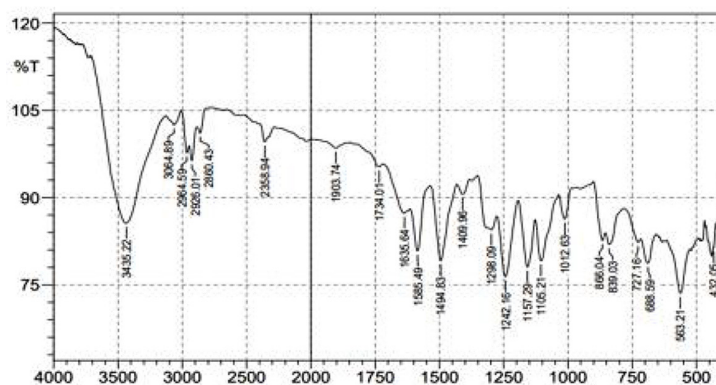


Figure 7. FTIR membrane polysulfone without ZIF-8 nanoparticles

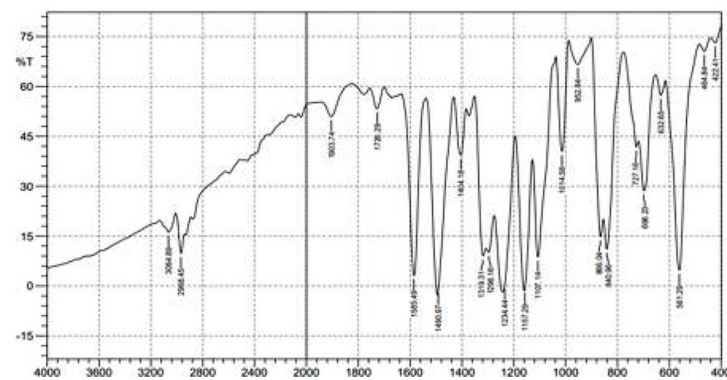
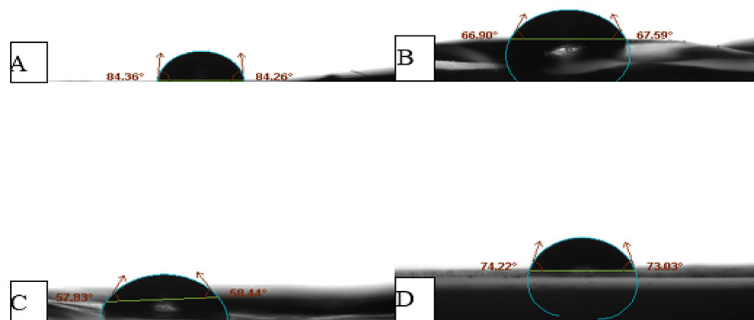


Figure 8. FTIR membrane polysulfone with ZIF-8 nanoparticles

## CONTACT ANGLE AND POROSITY ANALYSES OF MEMBRANES

The contact angle measurements for polysulfone (PSF) membranes under different circumstances are shown in Figure 9A. The hydrophobicity of the untreated PSF membrane is demonstrated by its average contact angle of  $73,62^\circ$ . The polymer's natural chemical structure, which includes sulfone groups and aromatic rings, gives it hydrophobic properties. The observed high contact angle results from these non-polar components' poor interaction with water molecules. Nevertheless, PSF is renowned for its remarkable oxidative, thermal, hydrolytic, and dimensional stability despite its hydrophobic character (Eren et al., 2015). Figure 9B show that upon the addition of ZIF-8 a highly porous structure, the contact angle decreases to  $67.29^\circ$ . The porous structure of ZIF-8 contains small pores that attract water molecules, thereby

improving the interaction between the membrane and water. This enhanced interaction effectively reduces the contact angle, making the membrane more (Ali et al., 2021). Figure 9C show that with further loading of ZIF-8, the contact angle decreases to  $58.13^\circ$ . The increase in the number of hydrophilic functional groups from ZIF-8 continues to enhance the interaction with water molecules (Sun et al., 2018). Figure 9D show that at higher ZIF-8 loading, the membrane surface becomes rougher, which can lead to a slight increase in hydrophobicity (Khan et al., 2020). The porosity of the membrane is influenced by various factors, including modifications made during manufacturing and the type of materials used. These factors can lead to an increase in membrane porosity. As shown in Figure 10, the PSU membrane, which is free from ZIF-8, has the lowest porosity at 50%. However, porosity increases progressively with the incorporation of ZIF-8 into the polymer matrix. Specifically, for



**Figure 9.** A) contact angle membrane without ZIF-8, B) contact angle membrane 0.0025 g from ZIF-8, C) contact angle membrane 0.005 g from ZIF-8, D) contact angle membrane 0.0075 g from ZIF-8

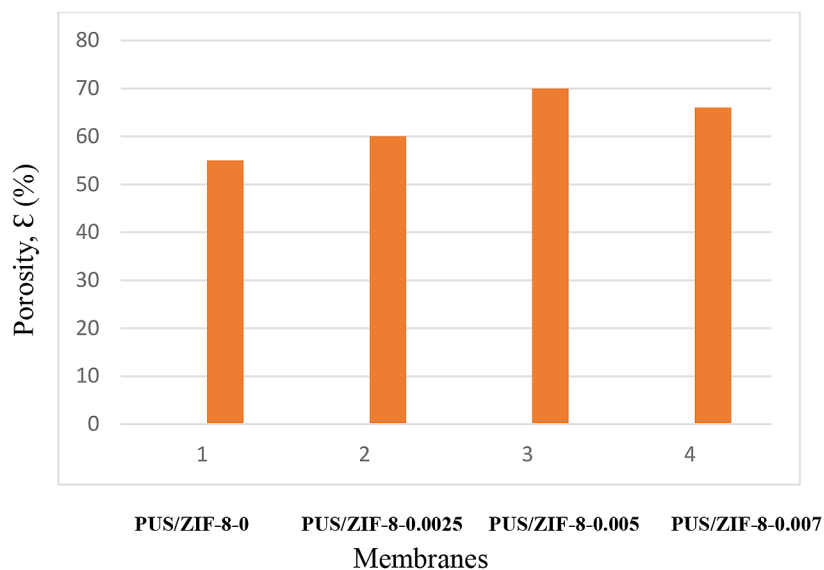


**Figure 10.** The porosity percentages of membranes

PSU/ZIF-8-0.025wt.%, the porosity rises to 60%, and for PSU/ZIF-8-0.05wt.%, it further increases to 70%. For PSU/ZIF-8-0.07wt.%, however, the porosity decreases to 66%. As the amount of ZIF-8 increases, agglomeration or clustering of ZIF-8 particles may occur within the polymer matrix. This clustering can block the pores or reduce the available void spaces between polymer chains, thereby decreasing the overall porosity (Wang et al., 2020). The agglomeration disrupts the uniform distribution of the material and forms dense regions that reduce pore formation (Yasir et al., 2024).

### MEMBRANE PERFORMANCE TEST

The current study focused on water flux and oil rejection to investigate how varying concentrations of ZIF-8 affected the filtering performance of a 14-weight percent polymer membrane. Membranes loaded with ZIF-8 were compared to membranes devoid of this porous material in terms of their mechanical and structural characteristics. Figure 11 illustrates the effect of ZIF-8 incorporation on the membrane performance. The water flux of the 14-weight percent polymer membrane without ZIF-8 increased from 50 L/m<sup>2</sup>·h at 0 pressure to 66.51 L/m<sup>2</sup>·h at 4 bar, while the rejection rate ranged from 86% to 89%. The membrane’s permeability has increased, but its ability to reject oil has somewhat decreased, as evidenced by the improvement in water flow. Water flux significantly increased from 53.57 L/m<sup>2</sup>·h at 0 bar to 75 L/m<sup>2</sup>·h at 4 bar upon the addition of 0.025 wt.% of ZIF-8 to the membrane. The rejection rate went from 87% to 86%, a little decline in spite of this improvement. This implies that including ZIF-8 enhances permeability while having a negligible effect on the membrane’s capacity to reject oils. The best results came when

0.05wt.% of ZIF-8 was added; the water flux rose from 53.57 L/m<sup>2</sup>·h at 0 pressure to 74.4 L/m<sup>2</sup>·h at 4 bar, while the rejection decreased somewhat from 98% to 96%. The large performance gain can be due to an optimal balance in pore size established by this amount of ZIF-8, which enhances water permeability while retaining a high level of oil rejection. The water flux increased from 20 L/m<sup>2</sup>·h to just 24.48 L/m<sup>2</sup>·h. when 0.075wt.% of ZIF-8 was added, and the rejection rate stayed between 97% and 96%. This implies that excessive pore expansion results from raising the ZIF-8 level to 0.075wt.%. decreasing the membrane’s overall effectiveness. Based on these results, it can be said that adding 0.05 wt.% of ZIF-8 produced the best results, achieving the ideal balance between oil rejection and water flux. These findings suggest that incorporating ZIF-8 into polymer membranes is a viable tactic to improve filtration efficiency in applications involving the separation of water and oil. When porous ZIF-8 is added, water flow or transport is improved (Masibi et al., 2022).

Table 2 shows a comparison between the polysulfone membrane with ZIF-8 and a few previously published membranes utilized for oil removal. The variations in the additives employed in these investigations are also highlighted in the table. Notably, ZIF-8 was employed as a nanomaterial in this study to increase membrane performance; however, no further additives were used to improve flux or oil rejection, which may be a topic for further investigation. In contrast to other research that used various chemicals to improve membrane performance, the membrane in this study demonstrated a greater water flux and equivalent oil rejection. The type of polymeric materials and additional nanomaterials greatly influence membrane performance, as certain materials may enhance oil resistance or water permeability.

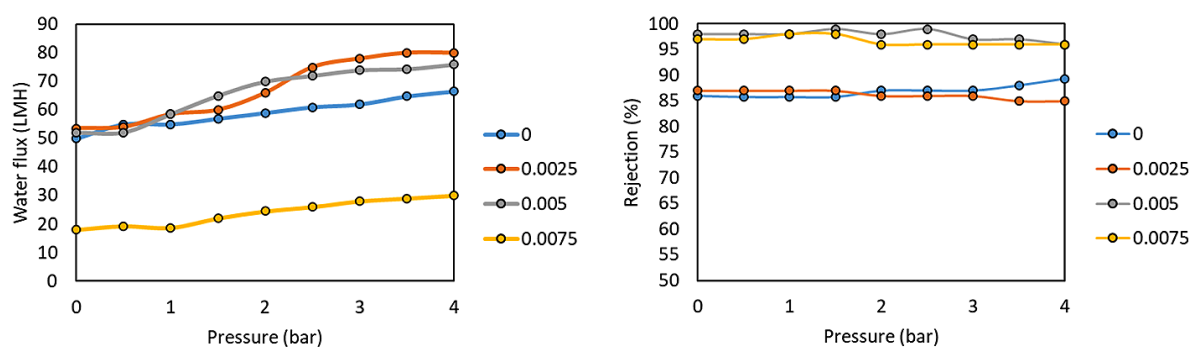


Figure 11. Water flux and rejection for PSU membranes in oily wastewater under operation conditions of (0 to 4) bar

**Table 2.** Comparison of oil/water emulsion separation performance

Material	Solvent	Concentration of precursor solution	Flux	Oil rejection (%)	Ref.
PAN@ZIF-8	(DMF) and methanol	(10wt.%PAN/16wt.%ZIF-8)/DMF	>900	>99.95	(Cai et al., 2017)
Au@ZIF-8@PAN-TD	(DMF), methanol, and water	16wt.%PAN+0.1wt.%f Au@ZIF-8NPs)/DM	>200	97.8%	(Zhang et al., 2019)
ZIF-8/PVDF	DMAc	PVDF/ Z1 (0.1 wt.%) PVDF/ Z2 (0.2 wt.%)	310 275	98% 76%	(Karimi et al., 2019)
ZIF-8/GO	TMC	PVDF 1.5 g/L of ZIF-8/GO 0.15% (w/v) of TMC	110 ± 6 L	99.99%	(Yue et al., 2020)
Nylon 6,6 NFM/ZIF-8	Formic and acetic acid	Nylon 6,6 formic and acetic acid (14:86)	1967	89%	(Abd Halim et al., 2019)
RC@PDA/ZIF-8	Tris-HCL		446.4	>99	(Xie et al., 2020)
ZIF-8			1411.8	> 99.99	(You et al., 2021)
ZIF-8-DMBIM			1643.1	99.95%	(You et al., 2021)
PVDF-g-ZIF-8	DMAC and acetone	PVDF (3.8 g) and 1.0 g of nano-ZnO, DMAC and acetone mixture solution, 4:1 v/v to a concentration of 12 wt. %	1.11	92.93%	(Xu et al., 2018)
Co – PDMS@ZIF- 8-coated MWCNT	THF	(PDMS (, THF a weight ratio of 10:1	170	99.97%	(Yang et al., 2020)
Cu(OH) <sub>2</sub> @ZIF-8	Methanol	Poly(vinylpyrrolidone)	90,000	97.2%	(Q. Li et al., 2018)
Cotton/ZIF-8 @ PDMS		Co-PDMS	n.d.	95 %	(Ye et al., 2019)
PSU/ZIF-8	DMF	(14wt.%PSU /ZIF-8)/DMF	35.17	98%	This work

## CONCLUSIONS

Membrane technology has been used in a number of processes, including oily wastewater treatment, water purification, and desalination. Because they can be completed quickly and easily. The majority of research so far has been on creating novel membranes. Contact angle, FTIR, SEM, and XRD were used to investigate the generated membrane and nanomaterial. The ZIF-8 nanomaterial's integration and influence on the shape and chemical structure of the generated membrane were confirmed by the characterization results. Measurements of hydrophilicity revealed a noticeable improvement, particularly with the increased ZIF-8 concentration of 0.005 g. Overall porosity and average roughness agreed well with the outcomes of the ultrafiltration examinations. A rejection of 98% was observed for membrane 0.05wt.%, whereas 86%, 87%, and 97% rejection rates were found in the oil-in-water separation experiments performed on membranes ZIF-8-0, ZIF-8-0.025 and ZIF-8-0.075. These results show that ZIF-8-modified membranes have the potential to enhance filtration performance in a range of water treatment applications, providing a viable option for effective separation procedures.

## REFERENCES

1. Abd Halim, N. S., Wirzal, M. D. H., Bilad, M. R., Md Nordin, N. A. H., Adi Putra, Z., Mohd Yusoff, A. R., Narkkun, T., Faungnawakij, K. (2019). Electrospun nylon 6, 6/ZIF-8 nanofiber membrane for produced water filtration. *Water*, 11(10), 2111. <https://doi.org/10.3390/w11102111>
2. Al-Furaiji, M. H., Arena, J. T., Chowdhury, M., Benes, N., Nijmeijer, A., McCutcheon, J. R. (2018). Use of forward osmosis in treatment of hyper-saline water. *Desalination and Water Treatment*, 133, 1–9. <https://doi.org/10.5004/dwt.2018.22851>
3. Al-Jadir, T., Alardhi, S. M., Alheety, M. A., Najim, A. A., Salih, I. K., Al-Furaiji, M., Alsally, Q. F. (2022). Fabrication and characterization of polyphenylsulfone/titanium oxide nanocomposite membranes for oily wastewater treatment. *Journal of Ecological Engineering*, 23(12). <https://doi.org/10.12911/22998993/154770>
4. Ali, M., Atta, A., Medhat, M., Shahat, A., Mohamed, S. (2021). Effective removal of methyl blue and crystal violet dyes using improved polysulfone/ZIF-8 nanocomposite ultrafiltration membrane. *Bio-interface Res. Appl. Chem*, 12, 7942-7956. <https://doi.org/10.33263/BRIAC126.79427956>
5. Arunachalam, M., Sinopoli, A., Aidoudi, F., Creager, S. E., Smith, R., Merzougui, B., Aïssa, B.

- (2021). Investigating the suitability of poly tetraarylphosphonium based anion exchange membranes for electrochemical applications. *Scientific reports*, 11(1), 13841. <https://doi.org/10.1038/s41598-021-93273-x>
6. Beaugerard, N., Al-Furaiji, M., Dias, G., Worthington, M., Suresh, A., Srivastava, R., Burkey, D. D., McCutcheon, J. R. (2020). Enhancing iCVD modification of electrospun membranes for membrane distillation using a 3D printed Scaffold. *Polymers*, 12(9), 2074. <https://doi.org/10.3390/polym12092074>
  7. Cai, Y., Chen, D., Li, N., Xu, Q., Li, H., He, J., Lu, J. (2017). Nanofibrous metal–organic framework composite membrane for selective efficient oil/water emulsion separation. *Journal of Membrane Science*, 543, 10–17. <https://doi.org/10.1016/j.memsci.2017.08.047>
  8. Cococceanu, A. L., & Man, T. E. (2021). Methods and Characteristics of Conventional Water Treatment Technologies. *Water Safety, Security and Sustainability: Threat Detection and Mitigation*, 305–330. <https://doi.org/10.1007/9>
  9. Costa, B. A., Abuçafy, M. P., Barbosa, T. W. L., da Silva, B. L., Fulindi, R. B., Isquibola, G., da Costa, P. I., & Chiavacci, L. A. (2023). ZnO@ ZIF-8 nanoparticles as nanocarrier of ciprofloxacin for antimicrobial activity. *Pharmaceutics*, 15(1), 259. <https://doi.org/10.3390/pharmaceutics15010259>
  10. Dasgupta, J., Sikder, J., Chakraborty, S., Curcio, S., Drioli, E. (2015). Remediation of textile effluents by membrane based treatment techniques: a state of the art review. *Journal of environmental management*, 147, 55–72. <https://doi.org/10.1016/j.jenvman.2014.08.008>
  11. Deng, Y., & Zhao, R. (2015). Advanced oxidation processes (AOPs) in wastewater treatment. *Current Pollution Reports*, 1, 167–176. <https://doi.org/10.1007/s40726-015-0015-z>
  12. Eren, E., Sarihan, A., Eren, B., Gumus, H., & Kocak, F. O. (2015). Preparation, characterization and performance enhancement of polysulfone ultrafiltration membrane using PBI as hydrophilic modifier. *Journal of Membrane Science*, 475, 1–8. <https://doi.org/10.1016/j.memsci.2014.10.010>
  13. Ji, Y., Qian, W., Yu, Y., An, Q., Liu, L., Zhou, Y., Gao, C. (2017). Recent developments in nanofiltration membranes based on nanomaterials. *Chinese Journal of Chemical Engineering*, 25(11), 1639–1652. <https://doi.org/10.1016/j.cjche.2017.04.014>
  14. Karimi, A., Khataee, A., Vatanpour, V., & Safarpour, M. (2019). High-flux PVDF mixed matrix membranes embedded with size-controlled ZIF-8 nanoparticles. *Separation and Purification Technology*, 229, 115838. <https://doi.org/10.1016/j.seppur.2019.115838>
  15. Khan, I. U., Othman, M. H. D., Jilani, A., Ismail, A., Hashim, H., Jaafar, J., Zulhairun, A., Rahman, M. A., & Rehman, G. U. (2020). ZIF-8 based polysulfone hollow fiber membranes for natural gas purification. *Polymer Testing*, 84, 106415. <https://doi.org/10.1016/j.polymertesting.2020.106415>
  16. Li, G., Yang, H., An, T., & Lu, Y. (2018). Antibiotics elimination and risk reduction at two drinking water treatment plants by using different conventional treatment techniques. *Ecotoxicology and environmental safety*, 158, 154–161 <https://doi.org/10.1016/j.ecoenv.2018.04.019>
  17. Li, Q., Deng, W., Li, C., Sun, Q., Huang, F., Zhao, Y., & Li, S. (2018). High-flux oil/water separation with interfacial capillary effect in switchable superwetting Cu(OH) 2@ ZIF-8 nanowire membranes. *ACS applied materials & interfaces*, 10(46), 40265–40273. <https://doi.org/10.1021/acsami.8b13983>
  18. Masibi, E. G., Makhetha, T. A., Moutloali, R. M. (2022). Effect of the Incorporation of ZIF-8@ GO into the Thin-Film Membrane on Salt Rejection and BSA Fouling. *Membranes*, 12(4), 436. <https://doi.org/10.3390/membranes12040436>
  19. Mei, X., Yang, S., Lu, P., Zhang, Y., & Zhang, J. (2020). Improving the selectivity of ZIF-8/polysulfone-mixed matrix membranes by polydopamine modification for H<sub>2</sub>/CO<sub>2</sub> separation. *Frontiers in Chemistry*, 8, 528. <https://doi.org/10.3389/fchem.2020.00528>
  20. Mulay, M. R., Martsinovich, N. (2023). Water pollution and advanced water treatment technologies. In *The Palgrave Encyclopedia of Urban and Regional Futures* (2184–2200). Springer. <https://doi.org/10.1007/9>
  21. Nawaz, M. S., Parveen, F., Gadelha, G., Khan, S. J., Wang, R., Hankins, N. P. (2016). Reverse solute transport, microbial toxicity, membrane cleaning and flux of regenerated draw in the FO-MBR using a micellar draw solution. *Desalination*, 391, 105–111. <https://doi.org/10.1016/j.desal.2016.02.023>
  22. Parsons, S. (2004). *Advanced oxidation processes for water and wastewater treatment*. IWA publishing.
  23. Rathi, B. S., & Kumar, P. S. (2021). Application of adsorption process for effective removal of emerging contaminants from water and wastewater. *Environmental Pollution*, 280, 116995. <https://doi.org/10.3390/w13091309>
  24. Rozkošný, M., Křiška, M., Šálek, J., Bodík, I., Istenič, D. (2014). Natural technologies of wastewater treatment. *Europe: Global Water Partnership Central and Eastern Europe*.
  25. Singh, R., & Hankins, N. P. (2016). Introduction to membrane processes for water treatment. *Emerging membrane technology for sustainable water treatment*, 15–52. <https://doi.org/10.1016/B978-0-444-63312-5.00002-4>

26. Sun, H., Tang, B., Wu, P. (2018). Hydrophilic hollow zeolitic imidazolate framework-8 modified ultrafiltration membranes with significantly enhanced water separation properties. *Journal of Membrane Science*, 551, 283–293. <https://doi.org/10.1016/j.memsci.2018.01.053>
27. Tsai, C.-W., Langner, E. H. (2016). The effect of synthesis temperature on the particle size of nano-ZIF-8. *Microporous and Mesoporous Materials*, 221, 8-13. <https://doi.org/10.1016/j.micromeso.2015.08.041>
28. Vinila, V., Jacob, R., Mony, A., Nair, H. G., Issac, S., Rajan, S., Nair, A. S., Satheesh, D., Isac, J. (2014). X-ray diffraction analysis of nano crystalline ceramic PbBaTiO<sub>3</sub>. *Crystal Structure Theory and Applications*, 3(03), 57. <https://doi.org/10.4236/csta.2014.33007>
29. Wang, X.-p., Hou, J., Chen, F.-S., Meng, X.-M. (2020). In-situ growth of metal-organic framework film on a polydopamine-modified flexible substrate for antibacterial and forward osmosis membranes. *Separation and Purification Technology*, 236, 116239. <https://doi.org/10.1016/j.seppur.2019.116239>
30. Xie, A., Cui, J., Yang, J., Chen, Y., Lang, J., Li, C., Yan, Y., Dai, J. (2020). Dual superlyophobic zeolitic imidazolate framework-8 modified membrane for controllable oil/water emulsion separation. *Separation and Purification Technology*, 236, 116273. <https://doi.org/10.1016/j.seppur.2019.116273>
31. Xu, S., Ren, L. F., Zhou, Q., Bai, H., Li, J., Shao, J. (2018). Facile ZIF-8 functionalized hierarchical micronanofiber membrane for high-efficiency separation of water-in-oil emulsions. *Journal of applied polymer science*, 135(27), 46462. <https://doi.org/10.1002/app.46462>
32. Yang, Y., Guo, Z., Huang, W., Zhang, S., Huang, J., Yang, H., Zhou, Y., Xu, W., Gu, S. (2020). Fabrication of multifunctional textiles with durable antibacterial property and efficient oil-water separation via in situ growth of zeolitic imidazolate framework-8 (ZIF-8) on cotton fabric. *Applied Surface Science*, 503, 144079. <https://doi.org/10.1016/j.apsusc.2019.144079>
33. Yasir, A. T., Benamor, A., Ba-Abbad, M., Hawari, A. H. (2024). Performance of polysulfone ultrafiltration membranes incorporating graphene oxide nanoparticles functionalized with different generations of poly (amido amine). *Journal of Water Process Engineering*, 60, 105095. <https://doi.org/10.1016/j.jwpe.2024.105095>
34. Ye, H., Chen, D., Li, N., Xu, Q., Li, H., He, J., Lu, J. (2019). Durable and robust self-healing superhydrophobic Co-PDMS@ ZIF-8-coated MWCNT films for extremely efficient emulsion separation. *ACS applied materials & interfaces*, 11(41), 38313–38320. <https://doi.org/10.1021/acsami.9b13539>
35. You, H., Shangkum, G. Y., Chammingkwan, P., Taniike, T. (2021). Surface wettability switching of a zeolitic imidazolate framework-deposited membrane for selective efficient oil/water emulsion separation. *Colloids and Surfaces A: Physicochemical and Engineering Aspects*, 614, 126204. <https://doi.org/10.1016/J.COLSURFA.2021.126204>
36. Yu, L., Han, M., He, F. (2017). A review of treating oily wastewater. *Arabian Journal of Chemistry*, 10, S1913-S1922. <https://doi.org/10.1016/j.arabjc.2013.07.020>
37. Yue, R.-Y., Guan, J., Zhang, C.-M., Yuan, P.-C., Liu, L.-N., Afzal, M. Z., Wang, S.-G., Sun, X.-F. (2020). Photoinduced superwetting membranes for separation of oil-in-water emulsions. *Separation and Purification Technology*, 241, 116536. <https://doi.org/10.1016/j.seppur.2020.116536>
38. Zhang, Y., Jia, Y., Li, M., Hou, L. A. (2018). Influence of the 2-methylimidazole/zinc nitrate hexahydrate molar ratio on the synthesis of zeolitic imidazolate framework-8 crystals at room temperature. *Scientific reports*, 8(1), 9597. <https://doi.org/10.1038/s41598-018-28015-7>
39. Zhang, Z., Yang, Y., Li, C., Liu, R. (2019). Porous nanofibrous superhydrophobic membrane with embedded Au nanoparticles for the integration of oil/water separation and catalytic degradation. *Journal of Membrane Science*, 582, 350–357. <https://doi.org/10.1016/j.memsci.2019.04.024>
40. Zhao, C., Zhou, J., Yan, Y., Yang, L., Xing, G., Li, H., Wu, P., Wang, M., Zheng, H. (2021). Application of coagulation/flocculation in oily wastewater treatment: A review. *Science of the Total Environment*, 765, 142795. <https://doi.org/10.1016/j.scitotenv.2020.142795>